

# Protein Kinase A, Ca<sup>2+</sup>/Calmodulin-Dependent Kinase II, and Calcineurin Regulate the Intracellular Trafficking of Myopodin between the Z-Disc and the Nucleus of Cardiac Myocytes<sup>∇</sup>

Christian Faul,<sup>1</sup> Ashwini Dhume,<sup>2</sup> Alison D. Schecter,<sup>2</sup> and Peter Mundel<sup>1\*</sup>

*Department of Medicine<sup>1</sup> and Zena and Michael A. Wiener Cardiovascular Institute,<sup>2</sup>  
Mount Sinai School of Medicine, New York, New York 10029*

Received 29 May 2007/Returned for modification 6 July 2007/Accepted 22 September 2007

**Spatial and temporal resolution of intracellular signaling can be achieved by compartmentalizing transduction units. Myopodin is a dual-compartment, actin-bundling protein that shuttles between the nucleus and the Z-disc of myocytes in a differentiation- and stress-dependent fashion. Importin  $\alpha$  binding and nuclear import of myopodin are regulated by serine/threonine phosphorylation-dependent binding of myopodin to 14-3-3. Here we show that in the heart myopodin forms a Z-disc signaling complex with  $\alpha$ -actinin, calcineurin, Ca<sup>2+</sup>/calmodulin-dependent kinase II (CaMKII), muscle-specific A-kinase anchoring protein, and myomegalin. Phosphorylation of myopodin by protein kinase A (PKA) or CaMKII mediates 14-3-3 binding and nuclear import in myoblasts. Dephosphorylation of myopodin by calcineurin abrogates 14-3-3 $\beta$  binding. Activation of PKA or inhibition of calcineurin in adult cardiac myocytes releases myopodin from the Z-disc and induces its nuclear import. The identification of myopodin as a direct target of PKA, CaMKII, and calcineurin defines a novel intracellular signaling pathway whereby changes in Z-disc dynamics may translate into compartmentalized signal transduction in the heart.**

A fundamental principle in cell biology is the propagation of diverse physiological responses by parallel signaling pathways that are assembled from a finite number of protein kinases and phosphatases (35). Given the existence of parallel signaling pathways, the spatial and temporal control of protein kinases and phosphatases is paramount for the selectivity and effectiveness of phosphorylation and dephosphorylation events (35). The subcellular compartmentalization of protein kinases and phosphatases by scaffolding proteins, such as A-kinase anchoring proteins (AKAPs), can effectively restrict signal transduction to specific sites within a cell (41). In fact, AKAPs have been shown to dynamically assemble different cyclic AMP (cAMP) effectors to control the cellular actions of cAMP spatially and temporally (39).

The Z-disc is a multiprotein complex which forms the lateral boundaries of the sarcomer, the contractile unit of striated muscle (5). The Z-disc serves as an anchor for thin filaments where antiparallel  $\alpha$ -actinin dimers, the major component of the Z-disc (38), cross-link neighboring actin polymers. Additionally, the Z-disc mechanically links the plasma membrane to the contractile machinery (10). For a long time it was assumed that the passive transmission of force generated within the myofilament system is the main function of the Z-disc. However, with the recent discovery of multiple novel proteins as Z-disc components, it became obvious that the Z-disc has not only structural and scaffolding functions but also participates in signal transduction events (13). In fact, multiple signaling molecules, including protein kinases (30), phosphatases (14), phos-

phodiesterases (30), small GTPases (25), G-proteins (24), adenylate cyclase (24), and the second messenger cAMP (44), were linked to the Z-disc. Some signaling proteins are in dynamic exchange between the Z-disc and the cytoplasm. They can display variable sarcomeric locations and shuttle between the Z-disc and the nucleus (25). The dynamic relocation of Z-disc proteins in response to stress or extracellular signals suggests that the Z-disc creates a giant communicative network that integrates signals from various origins. Work from several groups suggests that the Z-disc of cardiac myocytes serves as a mechanosensor in signal transduction during cardiac remodeling (22, 33). Mounting evidence supports the notion that the Z-disc can sense an increase in mechanical load and communicate with the nucleus to induce changes in gene expression, which in turn result in cardiac hypertrophy (9, 36).

Myopodin is a dual-compartment, actin-bundling protein that shuttles between the nucleus and the Z-disc of myocytes in a differentiation- and stress-dependent fashion (43). Under stress conditions, myopodin is depleted from the Z-disc and enters the nucleus (43). Recently we reported that importin  $\alpha$  binding and subsequent nuclear import of myopodin are regulated by the serine/threonine phosphorylation-dependent binding of myopodin to 14-3-3 (11). Here we show that myopodin participates in intracellular signal transduction between the Z-disc and the nucleus of differentiated adult cardiac myocytes. This pathway is regulated by protein kinase A (PKA), Ca<sup>2+</sup>/calmodulin-dependent kinase II (CaMKII), and calcineurin. We also provide evidence that 14-3-3 competes with  $\alpha$ -actinin for binding to myopodin and causes the release of myopodin from its Z-disc anchor,  $\alpha$ -actinin.

\* Corresponding author. Mailing address: Department of Medicine, Mount Sinai School of Medicine, One Gustave L. Levy Place, Box 1243, New York, NY 10029-6574. Phone: (212) 659-9332. Fax: (212) 849-2643. E-mail: peter.mundel@mssm.edu.

<sup>∇</sup> Published ahead of print on 8 October 2007.

## MATERIALS AND METHODS

**Cloning and vectors.** FLAG- and green fluorescent protein (GFP)-tagged mouse wild-type and mutant (S225A, T272A, S225D, T272E, S225AT272A, and

S225DT272E) myopodin as well as the FLAG- and glutathione *S*-transferase (GST)-14-3- $\beta$  constructs and FLAG-raver were described before (11). FLAG- $\alpha$ -actinin-2 was described before (1). Human myomegalin fragment (amino acids [aa] 1 to 171) was subcloned into pFLAG from the yeast two-hybrid prey vector pAct2 (BD Biosciences Clontech). Wild-type and constitutively active (aCnA; aa 1 to 397) calcineurin A $\alpha$  (kindly provided by Eric N. Olson) were subcloned into pEGFP-N1. Wild-type and constitutively active (H282R) GFP-CaMKII constructs were kindly provided by Thomas R. Soderling, and wild-type and truncated (aa 585 to 1286) GFP-muscle-specific AKAP (mAKAP) was provided by John D. Scott.

**Yeast two-hybrid screen.** The mouse myopodin fragments Myo-1 (aa 1 to 186), Myo-2 (187 to 420), Myo-3 (421 to 554), and Myo-4 (555 to 757) were used to screen pretransformed mouse embryonic (embryonic day 17.5) or human heart muscle Matchmaker cDNA libraries (Matchmaker Two-Hybrid System 3; Clontech) as described before (11).

**Cell culture and transfection.** Cell cultures of C2C12 myoblasts (ATCC) and HEK293 cells (ATCC) as well as transient transfections using Lipofectamine 2000 (Invitrogen) were done as previously described (11). H89 and KN62 (Sigma-Aldrich) were applied at a final concentration of 10  $\mu$ M for 6 h to cultured cells, and Rp-adenosine 3',5'-cyclic monophosphorothioate triethylammonium (Rp-cAMP), KT5720, wortmannin, and Ro31-8220 (all from Sigma-Aldrich) were used at 1  $\mu$ M for 6 h. Primary cultures of calcium-tolerant rat ventricular cardiac myocytes were prepared from 6- to 8-week-old Sprague-Dawley rats as recently described (37). Briefly, the animals were heparinized and the hearts were retrograde perfused for 5 min at 37°C with perfusion buffer containing, in mmol/liter: 120.4 NaCl, 14.7 KCl, 0.6 KH<sub>2</sub>PO<sub>4</sub>, 0.6 NaHPO<sub>4</sub>, 1.2 MgSO<sub>4</sub>, 10 Na-HEPES, 4.6 NaHCO<sub>3</sub>, 30 taurine, 10 2,3-butanedione monoxime, and 5.5 glucose; pH 7.0. Then, the perfusate was switched to an enzyme solution containing collagenase (2.4 mg/ml; 258  $\mu$ g/mg; Worthington type II), and the hearts were perfused for another 8 min. Ventricular tissue was finely minced and gently shaken in enzyme solution for 2 min before stop buffer containing 10% fetal bovine serum (FBS) and 12.5 mM CaCl<sub>2</sub> was added. After filtering through a nylon mesh, the cardiac myocytes were made Ca<sup>2+</sup> tolerant over 15 min. The cells were resuspended in myocyte plating medium (minimal essential medium, 10% FBS, 10 mM 2,3-butanedione monoxime, 100 units/ml penicillin, 2 mM glutamine) and plated at a density of  $2 \times 10^4$  cells/ml onto coverslips precoated with laminin or coverslip-bottom culture slides (2  $\mu$ g/cm<sup>2</sup>; Invitrogen). After 2 h the medium was changed to short-term culture medium (minimal essential medium, 0.1% bovine serum albumin, 100 units/ml penicillin, 2 mM glutamine). Cardiac myocytes were cultured overnight at 37°C in 2% CO<sub>2</sub> before 400 nM CsA or a combination of 20  $\mu$ M forskolin and 100  $\mu$ M 3-isobutyl-1-methylxanthine (IBMX) (all from Sigma-Aldrich) was added for 2 h.

**Antibodies.** Rabbit anti-myopodin antibody has been previously described (43). Rabbit anti-14-3- $\beta$  (C-20) antibody was from Santa Cruz Biotechnology, and mouse monoclonal anti- $\alpha$ -actinin antibody (sarcomeric, clone EA-53) was from Sigma-Aldrich. Rabbit anti-mAKAP and goat anti-PKA-RII were from Upstate, and rabbit anti-CaMKII (pThr305) was from Sigma-Aldrich. Anti-FLAG, anti-GFP, and anti-GST antibodies and anti-FLAG-M2 antibody covalently attached to agarose (Sigma-Aldrich), as well as horseradish peroxidase and fluorochrome-coupled secondary antibodies were described before (11).

**Immunofluorescence microscopy and quantification of subcellular myopodin localization.** Frozen sections of mouse hearts were prepared for immunohistochemical analysis as described before (43). For immunocytochemistry, C2C12 myoblasts and isolated cardiac myocytes were fixed and immunolabeled as described previously (11). Images were captured using epifluorescence on a DMI 6000B microscope (Leica) and evaluated by deconvolution software (Leica) as described before (2). For quantification, the cells were divided into three groups dependent on the subcellular localization of the visualized protein: majority in the nucleus (N>C), majority in the cytoplasm (N<C), or equal nuclear-cytoplasmic distribution (N=C), as described by others (40). For each group, 100 cells were analyzed in a blind fashion. The results of three independent experiments are expressed as means  $\pm$  standard deviations and were assessed by Student's *t* test or analysis of variance (ANOVA).

**Western blotting, immunoprecipitation, and GST binding assays.** Sodium dodecyl sulfate-polyacrylamide gel electrophoresis (SDS-PAGE), Western blotting, and coimmunoprecipitation of FLAG- and GFP-tagged fusion proteins from transfected HEK293 cells were done as described before (11). To immunoprecipitate endogenous protein complexes from mouse heart (11), protein extraction was carried out at 4°C in a tight-fitting Potter homogenizer with 20 strokes at 1,300 rpm in 10 volumes of T-PER tissue protein extraction reagent (Pierce) supplemented with Complete Mini protease inhibitor cocktail (Roche). The purification of GST, GST-14-3- $\beta$ , and GST- $\alpha$ -actinin-2 from bacteria and the purification of FLAG-myopodin, FLAG-14-3- $\beta$ , and FLAG- $\alpha$ -actinin-2

from HEK293 cells were done as previously described (11). For the reconstitution of interactions between GST- and FLAG-fusion proteins, 1  $\mu$ g of GST fusion protein was immobilized on glutathione-agarose beads (Sigma-Aldrich). Beads were washed five times in 1% Triton X-100 in phosphate-buffered saline, and 1  $\mu$ g of purified FLAG-fusion protein in 500  $\mu$ l Triton buffer (50 mM Tris pH 7.5, 150 mM NaCl, 1% Triton X-100) was added. For competition assays, 0, 100, 250, 500, or 1,000 ng of a second FLAG protein was added to the reaction mixture. Reaction mixtures were incubated under rotation for 2 h at 4°C, and beads were washed five times in Triton buffer. Proteins were eluted in 100  $\mu$ l sample buffer and analyzed by SDS-PAGE and immunoblotting (2).

**In vitro protein phosphorylation and dephosphorylation.** The recombinant catalytic subunit of PKA, the truncated monomer (aa 1 to 325) of the CaMKII  $\alpha$  subunit, and  $\lambda$  protein phosphatase ( $\lambda$ -PPase) were purchased from New England Biolabs, and purified CnA was from Promega. Recombinant FLAG-myopodin was purified from HEK293 cells and dephosphorylated with  $\lambda$ -PPase as described before (11). For in vitro phosphorylation, FLAG-myopodin was eluted from anti-FLAG beads with FLAG-M2 peptide (500  $\mu$ g/ml in phosphate-buffered saline), and 500 ng of FLAG-myopodin was incubated with 2,500 units of PKA or 120 units of activated CaMKII in the presence of 100 Ci/mol [ $\gamma$ -<sup>32</sup>P]ATP and 0.2 mM ATP at 30°C for 0 to 60 min. To analyze the dephosphorylation of myopodin, purified FLAG-myopodin from HEK293 cells was bound to FLAG-beads and dephosphorylated with  $\lambda$ -PPase as described before (11). Beads were washed three times in radioimmunoprecipitation assay buffer, and immobilized myopodin was radiolabeled by in vitro phosphorylation using PKA or CaMKII as described above. FLAG-myopodin was eluted from the FLAG-beads and incubated with 1 or 2 units of calcineurin, 3  $\mu$ M calmodulin, and reaction buffer or 100 units of  $\lambda$ -PPase at 30°C for 30 or 60 min. All reactions were performed in a total volume of 25  $\mu$ l and stopped by boiling in Laemmli buffer. A 20- $\mu$ l aliquot of each reaction mixture was analyzed by SDS-PAGE and phospho-imaging, and 5  $\mu$ l of each reaction mixture was analyzed by SDS-PAGE and immunoblotting using an anti-FLAG antibody (11). For quantification, the <sup>32</sup>P signal and the enhanced chemiluminescence signal of the immunoprecipitated FLAG-proteins were measured with ImageQuant TL software (Amersham Biosciences). Then, the <sup>32</sup>P signal/FLAG signal ratio was calculated, and the ratios for the wild-type or control reactions were defined as 100%. The results of three independent experiments are expressed as means  $\pm$  standard deviations and were assessed by Student's *t* test or ANOVA.

**In vivo protein phosphorylation and dephosphorylation.** HEK293 cells were transfected with FLAG-myopodin constructs and further cultured for 1 day. At 12 h before the experiment, cells were serum starved followed by incubation in phosphate-free Dulbecco's modified Eagle's medium for 2 h. Then, 0.2 mCi orthophosphate (<sup>32</sup>P in HCl), 20  $\mu$ l 1 M HEPES pH 7.4, and 200  $\mu$ l FBS were added to each well. Cells were further incubated at 37°C for 2 h before immunoprecipitation, followed by SDS-PAGE and phospho-imaging. To block PKA or CaMKII activities in cells, H89 or KN62 (10  $\mu$ M each) was added separately or together to serum- and phosphate-free medium. In some experiments, the in vivo labeling of myopodin was assessed in HEK293 cells after transient transfection with GFP-tagged constitutively active calcineurin or constitutively active CaMKII 24 h prior to the experiment. GFP served as a negative control. The quantitative analysis was conducted as described above.

## RESULTS

**Myopodin forms a novel Z-disc signaling unit with mAKAP, calcineurin, CaMKII, myomegalin, and  $\alpha$ -actinin.** We reported previously that importin  $\alpha$  binding and the subsequent nuclear import of myopodin are regulated by the serine/threonine phosphorylation-dependent binding of myopodin to 14-3-3 (11). However, the protein kinase(s) and phosphatase(s), which regulate the phosphorylation and dephosphorylation of myopodin, have not been determined. To identify signaling pathways that control the phosphorylation state of myopodin in the heart, we screened a human heart cDNA library using the yeast two-hybrid system as described before (11). Among several others, we identified mAKAP (19), myomegalin (42), and the catalytic subunit of calcineurin (CnA $\beta$ ) (21) as myopodin-interacting proteins. To confirm the yeast two-hybrid results with an independent biochemical approach, myopodin and its interacting proteins were coexpressed as FLAG- and

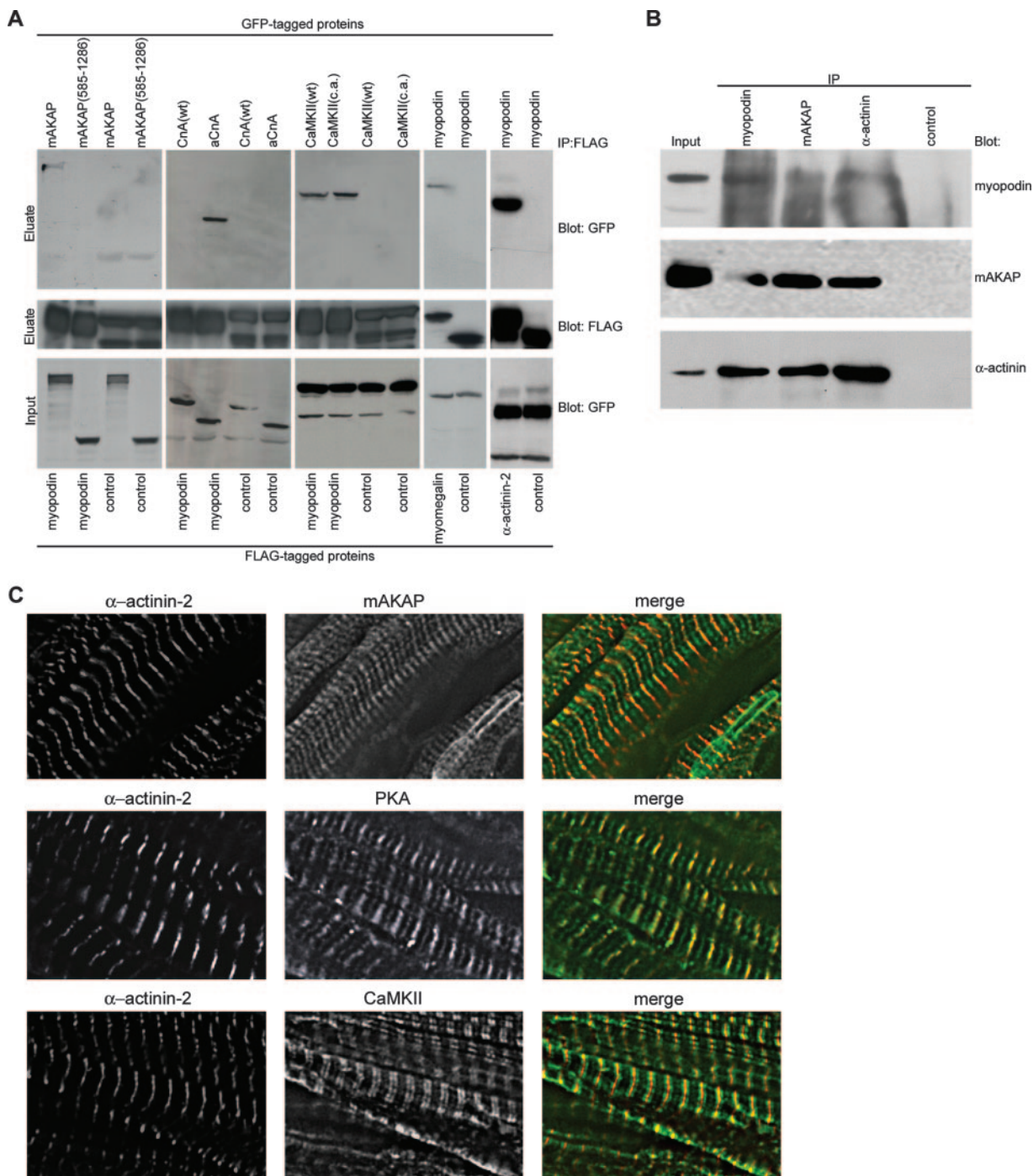


FIG. 1. Identification of a myopodin-containing signaling complex at the Z-disc in the heart. (A) GFP-tagged mAKAP, aCnA, and CaMKII coprecipitate with FLAG-myopodin from cotransfected HEK cells. No interaction is seen with the mAKAP fragment 585-1286 or wild-type CnA. GFP-fusion proteins do not bind FLAG-raver, which served as a negative control. Immunoprecipitation of FLAG-myomegalin (aa 1 to 171) or FLAG-alpha-actinin-2, but not FLAG-raver (control), specifically coprecipitate GFP-myopodin. (B) Coimmunoprecipitation experiments showing that endogenous myopodin interacts with mAKAP (middle panels) and alpha-actinin (lower panels) in adult mouse heart. Immunoprecipitations (IPs) were done with antimyopodin, anti-mAKAP, or anti-alpha-actinin, or with anti-GFP, serving as a negative control. (C) Deconvolution double-labeling immunofluorescence microscopy with alpha-actinin reveals the Z-disc localization of mAKAP, PKA, and CaMKII in adult mouse heart. CaMKII localizes to the Z-I junction embracing the alpha-actinin labeling. All three proteins can also be detected at the M-line. In addition, mAKAP displays perinuclear labeling.

GFP-fusion proteins in HEK293 cells and immunoprecipitated with anti-FLAG beads (Fig. 1A). FLAG-myopodin specifically interacted with full-length GFP-mAKAP, but not with the mAKAP fragment aa 585 to 1286 (19) comprising the spectrin

repeats that anchor mAKAP at the nucleus (Fig. 1A). Additionally, FLAG-myopodin specifically interacted with GFP-tagged autoactive CnA (aCnA) (32) but not wild-type GFP-CnA. No binding was found with FLAG-raver, which served

as a negative control. We also detected a specific interaction between FLAG-myomegalin (aa 1 to 171) and GFP-myopodin (Fig. 1A), thereby confirming the yeast two-hybrid results.

Database searches using PhosphoBase (<http://phospho.elm.eu.org>) suggested that the 14-3-3-binding motifs of myopodin (11) serve as CaMKII substrates. Therefore, we tested the hypothesis that myopodin can bind to CaMKII. FLAG-myopodin copurified with wild-type and constitutively active GFP-CaMKII (c.a.) from cotransfected HEK293 cells (Fig. 1A), suggesting a direct interaction between myopodin and CaMKII. We reported previously that the myopodin homologue synaptopodin interacts with  $\alpha$ -actinin-2 and  $\alpha$ -actinin-4 (1). Therefore, we tested whether both proteins also interacted with myopodin in cotransfected HEK cells. We observed that GFP-myopodin specifically interacted with FLAG- $\alpha$ -actinin-2 (Fig. 1A) and FLAG- $\alpha$ -actinin-4 (data not shown). The interactions between myopodin and its binding partners were further confirmed by endogenous coimmunoprecipitation studies with adult mouse heart extracts (Fig. 1B). Antimyopodin precipitated myopodin, and it also coprecipitated mAKAP and  $\alpha$ -actinin (Fig. 1B). Conversely, anti-mAKAP and anti- $\alpha$ -actinin coprecipitated myopodin (Fig. 1B), showing that the three proteins form a complex in the heart. No interactions were found with an irrelevant control antibody.

Previously, we have shown that in the adult heart myopodin colocalizes with  $\alpha$ -actinin at the Z-disc (43). To determine the subcellular localization of the identified myopodin-binding proteins, we performed double immunolabeling deconvolution microscopy on sections from adult mouse heart with the Z-disc-specific marker  $\alpha$ -actinin. mAKAP displayed a perinuclear distribution as described previously (19) but also colocalized with  $\alpha$ -actinin at the Z-disc (Fig. 1C, upper panels). PKA was detectable at the M-line, as was expected (30), but also with a greater intensity at the Z-disc, where it colocalized with  $\alpha$ -actinin (Fig. 1C, middle panels). CaMKII was detected at the M-line and even more strongly at the Z-I junction, where it flanked the  $\alpha$ -actinin labeling but did not overlap with it (Fig. 1C, lower panels). Collectively these data show that myopodin,  $\alpha$ -actinin, mAKAP, PKA, CaMKII, calcineurin, and myomegalin form a multimeric protein complex in the heart.

**PKA and CaMKII phosphorylate serine 225 and threonine 272 of myopodin in vitro.** Myopodin contains two functional 14-3-3-binding sites (RSLAS<sub>225</sub>VP and RSVT<sub>272</sub>SP), and binding of myopodin to 14-3-3 $\beta$  requires the phosphorylation of serine 225 (S225) and threonine 272 (T272) (11). Consensus 14-3-3-binding motifs (RSxpS/TxP and RxxxpS/TxP) serve as substrates for a variety of serine/threonine protein kinases, including PKA and CaMKII (8). Together with the fact that myopodin interacts with CaMKII and the PKA-anchoring protein mAKAP, thereby bringing myopodin in close proximity to PKA, the intriguing possibility that myopodin is a direct substrate of PKA and CaMKII needs to be considered. To test whether PKA and CaMKII can phosphorylate the phospho-acceptor sites S225 and T272 within the two 14-3-3-binding sites of myopodin, purified FLAG-myopodin was dephosphorylated with  $\lambda$ -PPase as described before (11) and then incubated with either PKA or CaMKII in the presence of [ $\gamma$ -<sup>32</sup>P]ATP (Fig. 2A). Both kinases phosphorylated myopodin, and increasing levels of [<sup>32</sup>P]myopodin were detected over time by phospho-imaging (Fig. 2A, left panel). In contrast, the

inactivation of the two phospho-acceptor sites in FLAG-myopodin by alanine substitutions (S225AT272A) (11) significantly decreased the phosphorylation of myopodin by PKA (Fig. 2A, upper right panel). Virtually no [<sup>32</sup>P]myopodin could be detected after incubation of S225AT272A with CaMKII, even after 60 min (Fig. 2A, lower panel). The quantitative analysis revealed a  $52.54 \pm 5.77\%$  reduction for PKA ( $P < 0.005$ , Student's *t* test) and a  $96.10 \pm 1.47\%$  reduction for CaMKII ( $P < 0.00001$ , Student's *t* test). The presence of equal amounts of FLAG-myopodin in each reaction mixture was confirmed by immunoblotting with anti-FLAG. These results demonstrate that PKA and CaMKII can phosphorylate S225 and T272 within the two 14-3-3-binding motifs of myopodin in vitro.

**PKA and CaMKII phosphorylate S225 and T272 of myopodin in vivo.** To explore the phosphorylation of myopodin in vivo, HEK293 cells were transfected with FLAG-myopodin and incubated in phosphate-free medium for 2 h followed by the addition of orthophosphate (<sup>32</sup>P) to the medium and further incubation for 2 h. FLAG-myopodin was immunoprecipitated, and <sup>32</sup>P labeling of myopodin was visualized by phospho-imaging. Compared to wild-type myopodin, S225AT272A showed a  $43.35 \pm 10.10\%$  ( $P < 0.02$ , Student's *t* test) reduction of <sup>32</sup>P labeling (Fig. 2B, left panels), demonstrating that S225 and T272 serve as phospho-acceptor sites in vivo. To test whether PKA and CaMKII can phosphorylate myopodin in vivo, wild-type FLAG-myopodin was expressed in HEK293 cells as described above and incubated for 2 h with <sup>32</sup>P in the presence of the PKA inhibitor H89 (10  $\mu$ M), the CaMKII inhibitor KN62 (10  $\mu$ M), or a combination of both. Compared to untreated cells, the inhibition of PKA and CaMKII significantly reduced <sup>32</sup>P labeling of FLAG-myopodin (Fig. 2B, middle panels). The quantification (60-min time point) showed a  $47.11 \pm 18.11\%$  reduction of wild-type myopodin for H89, a  $24.69 \pm 27.83\%$  reduction for KN62, and a  $90.92 \pm 2.81\%$  reduction for the combination of H89 and KN62 compared to the control ( $P < 0.0001$ , ANOVA). Compared to the control, H89 did not further decrease the <sup>32</sup>P labeling of S225AT272A ( $7.76 \pm 15.76\%$  reduction) ( $P$  value not significant), showing that S225 and T272 function as phosphorylation sites for PKA in vivo. In contrast, KN62 (Fig. 2B, right panels) further reduced the <sup>32</sup>P labeling of S225AT272A ( $65.56 \pm 12.38\%$ ), indicating that myopodin contains additional CaMKII sites outside its 14-3-3-binding motifs. The highest reduction of S225AT272A phosphorylation was detected when both kinase inhibitors were applied in combination ( $91.67 \pm 2.18\%$ ) ( $P < 0.000001$ , ANOVA). To further prove that CaMKII phosphorylates myopodin in vivo, HEK293 cells were cotransfected with FLAG-myopodin and GFP-tagged CaMKII (c.a.) and cultured in the presence of <sup>32</sup>P (see Fig. 4B, below). We detected a  $14.26 \pm 5.32\%$  increase ( $P < 0.05$ , Student's *t* test) in <sup>32</sup>P labeling of myopodin in the presence of GFP-CaMKII (c.a.) compared to the GFP control. Altogether, these results show that PKA and CaMKII can phosphorylate myopodin in vivo.

**Phosphorylation of myopodin by PKA or CaMKII mediates 14-3-3 binding.** To test whether the phosphorylation by PKA or CaMKII regulates the binding of myopodin to 14-3-3 $\beta$ , FLAG-myopodin was dephosphorylated with  $\lambda$ -PPase and rephosphorylated with PKA or CaMKII (Fig. 2C, left panel).

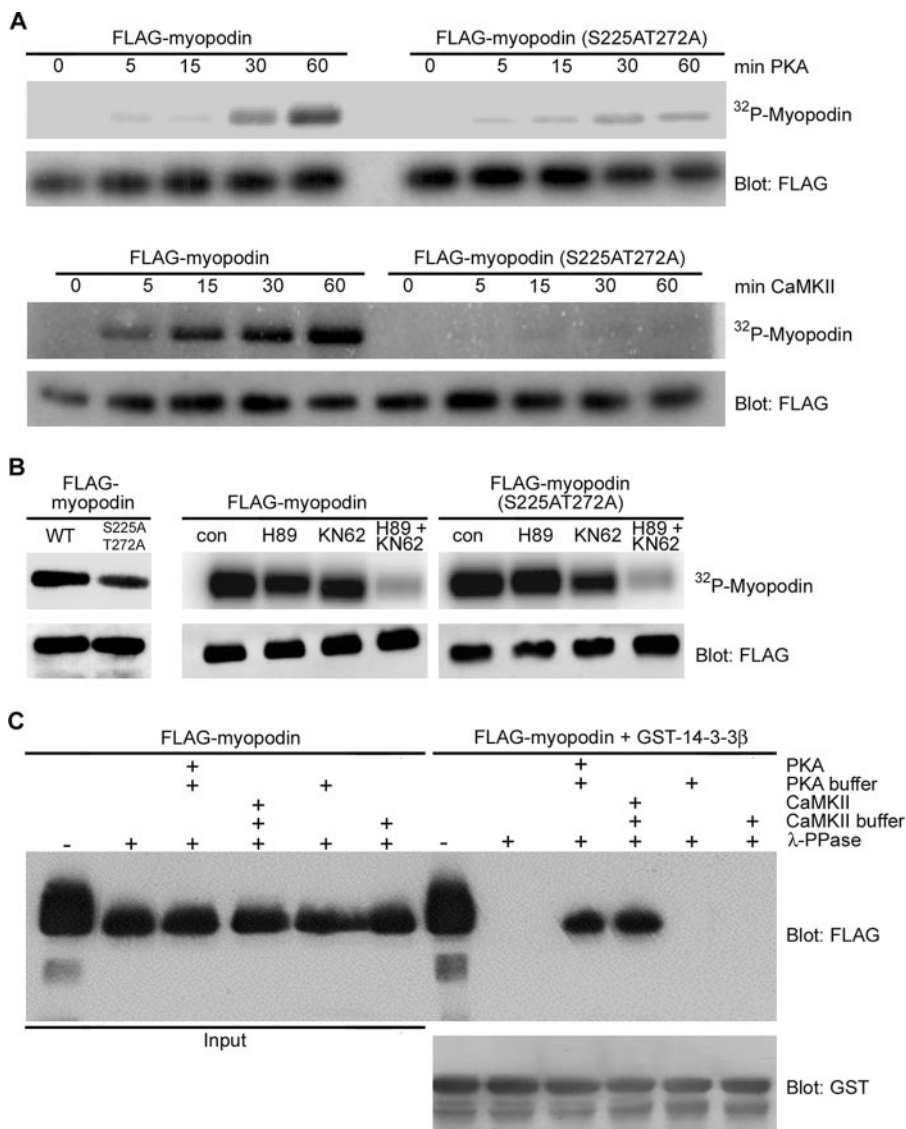


FIG. 2. Phosphorylation of myopodin by PKA and CaMKII mediates 14-3-3 binding. (A) Time-dependent in vitro phosphorylation of purified FLAG-myopodin by PKA (upper panels) and CaMKII (lower panels). Immunoblotting with anti-FLAG shows equal protein loading. Alanine substitution of S225 and T272 (S225AT272A) significantly reduces <sup>32</sup>P labeling of myopodin, indicating that both residues are phosphorylation sites for PKA and CaMKII. (B) Immunoprecipitation of in vivo-phosphorylated FLAG-myopodin from transfected HEK293 cells. Wild-type (WT) myopodin shows stronger <sup>32</sup>P labeling than S225AT272A (left panels). The inhibition of PKA by H89 or CaMKII by KN62 decreases <sup>32</sup>P labeling of WT FLAG-myopodin, showing that both kinases phosphorylate myopodin in vivo (middle panels). H89 does not further decrease <sup>32</sup>P labeling of S225AT272A (right panel), whereas KN62 reduces <sup>32</sup>P labeling of S225AT272A, indicating the presence of additional CaMKII sites in myopodin. Combined application of H89 and KN62 causes the highest reduction in <sup>32</sup>P labeling of wild-type and mutant myopodin. (C) In vitro phosphorylation of dephosphorylated (+λ-PPase) FLAG-myopodin (left panel) by PKA or CaMKII restores 14-3-3 binding of myopodin (right panels). Incubation with kinase reaction buffers alone does not restore the myopodin–14-3-3β interaction.

Then, purified GST–14-3-3β was incubated with 1 μg of purified FLAG-myopodin, and myopodin binding was analyzed by immunoblotting using an anti-FLAG antibody (Fig. 2C, right panel). Consistent with previous findings (11), dephosphorylation of myopodin with λ-PPase abrogated the myopodin–14-3-3β interaction, which was restored after rephosphorylation by PKA or CaMKII (Fig. 2C). No 14-3-3 binding was detected when myopodin was incubated in kinase reaction buffers without enzymes (Fig. 2C). The presence of only one functional 14-3-3-binding site within myopodin results in a decrease of

14-3-3 binding (11). To further analyze 14-3-3 binding of myopodin after PKA or CaMKII treatment and to determine the PKA and CaMKII phosphorylation sites in the two 14-3-3 motifs, we repeated the experiment with the FLAG-myopodin mutants S225A, T272A, and S225AT272A (Fig. 3). PKA-mediated phosphorylation of the single mutants S225A and T272A after λ-PPase treatment caused weak 14-3-3 binding compared to wild-type myopodin (Fig. 3, left panel), showing that both residues (S225 and T272) are PKA substrates. In contrast, CaMKII could only restore weak 14-3-3 binding in

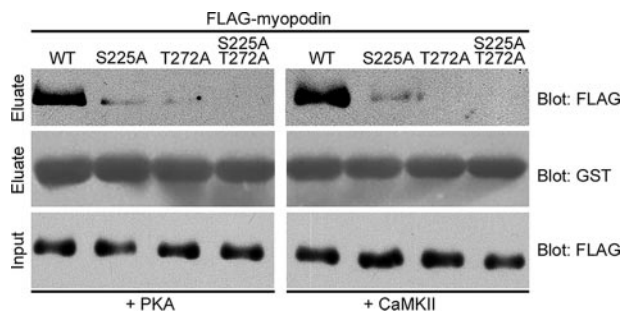


FIG. 3. S225 and T272 serve as PKA substrates, but only T272 serves as a CaMKII substrate. PKA phosphorylation of the single FLAG-myopodin mutants S225A and T272A after  $\lambda$ -PPase treatment causes weak binding to GST-14-3-3 $\beta$  (left panels). In contrast, only S225A, and not T272A, binds to GST-14-3-3 after CaMKII treatment, indicating that T272 but not S225 serves as a CaMKII phosphorylation site.

the S225A but not in the T272A mutant (Fig. 3, right panel), thereby demonstrating that T272, but not S225, is a CaMKII phosphorylation site. As expected from previous results (11), both protein kinases could not rescue 14-3-3 binding of S225AT272A, because both residues are required for the interaction (11).

**Calcineurin dephosphorylates myopodin in vitro and in vivo.** Consensus 14-3-3-binding motifs can be dephosphorylated by serine/threonine protein phosphatases, including calcineurin (8). In the current studies we identified the catalytic subunit of calcineurin (CnA) as a myopodin-interacting protein (Fig. 1A). To test whether calcineurin can dephosphorylate myopodin in vitro, purified FLAG-myopodin was dephosphorylated with  $\lambda$ -PPase and then rephosphorylated with PKA in the presence of [ $\gamma$ - $^{32}$ P]ATP. The  $^{32}$ P-labeled myopodin was then dephosphorylated with CnA for either 30 or 60 min (Fig. 4A, right panel). As a positive control, myopodin was dephosphorylated with  $\lambda$ -PPase (Fig. 4A, left panel) as previously described (11). Both phosphatases dephosphorylated myopodin, and decreasing levels of  $^{32}$ P-labeled myopodin were detected in a concentration-dependent manner compared to untreated [ $^{32}$ P]myopodin. In contrast, the incubation of [ $^{32}$ P]myopodin in reaction buffer without phosphatases did not result in a decrease in the  $^{32}$ P labeling. These data support that the phosphorylation of myopodin is stable over time and that its decrease specifically resulted from the phosphatase activity. To analyze the dephosphorylation of myopodin in vivo, FLAG-myopodin was coexpressed with GFP-aCnA in HEK293 cells and cultured in the presence of  $^{32}$ P. Radioactive labeling of myopodin was significantly reduced ( $93.67 \pm 2.34\%$ ,  $P = 0.0$ ,

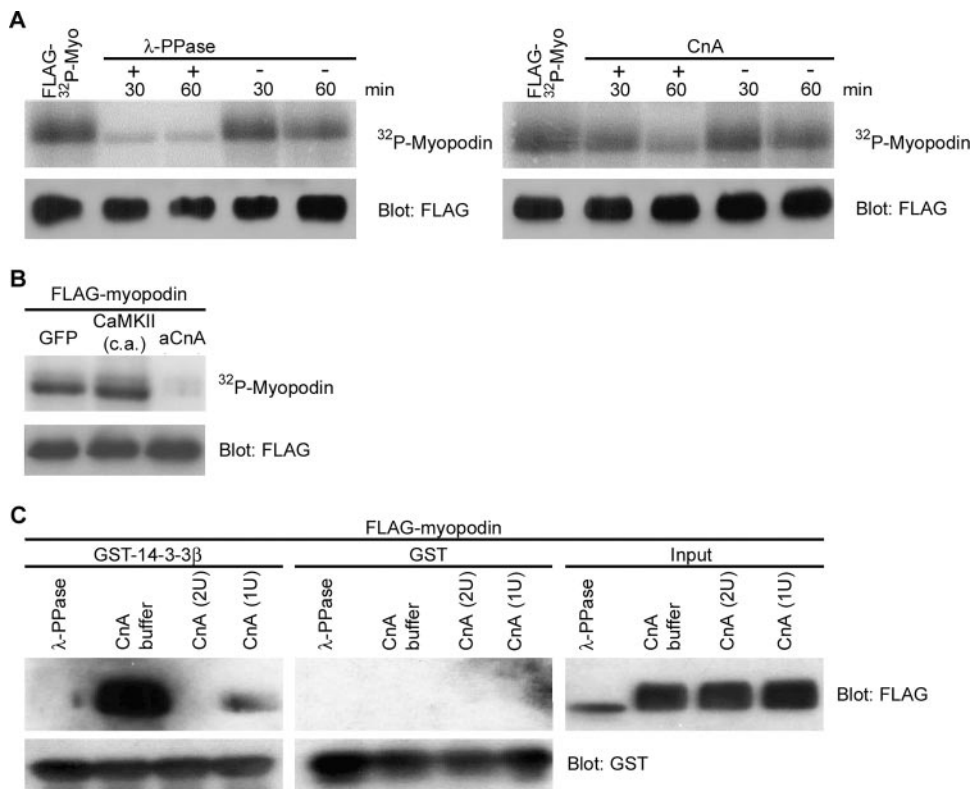


FIG. 4. Dephosphorylation of myopodin by calcineurin abrogates 14-3-3 binding. (A) Time-dependent in vitro dephosphorylation of purified  $^{32}$ P-labeled FLAG-myopodin by  $\lambda$ -PPase (left panel) or CnA (right panel). In the absence of phosphatases, [ $^{32}$ P]myopodin levels remain stable over time. The anti-FLAG blot shows equal protein loading. (B) In vivo phosphorylation of FLAG-myopodin in HEK293 cells is increased by cotransfections with autoactive GFP-CaMKII (c.a.) compared to the GFP control. Coexpression of constitutively active GFP-CnA (aCnA) almost completely abrogates the in vivo phosphorylation of myopodin (right lane). The anti-FLAG blot shows equal protein loading. (C) In vitro dephosphorylation of purified FLAG-myopodin with  $\lambda$ -PPase or CnA causes the concentration-dependent loss of GST-14-3-3 $\beta$  binding. In contrast, after incubation with CnA buffer alone, the myopodin-14-3-3 $\beta$  interaction is preserved. No myopodin binding is seen with GST alone (middle panels).

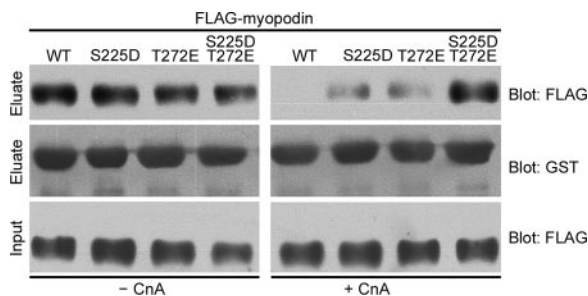


FIG. 5. S225 and T272 of myopodin serve as calcineurin substrates. FLAG-myopodin mutants S225D, T272E, and S225DT272E bind GST-14-3- $\beta$  in the absence of calcineurin (- CnA; left panels). In contrast, calcineurin treatment (+ CnA; right panels) abrogates 14-3-3 binding to wild-type myopodin (WT) while the interaction with S225DT272E is preserved. The reductions of 14-3-3 binding of S225D and T272E after CnA treatment show that both residues serve as calcineurin substrates.

Student's *t* test) (Fig. 4B, right lane) compared to myopodin immunoprecipitated from cells coexpressing GFP (Fig. 4B, left lane). These data demonstrate that the physiologically relevant protein phosphatase calcineurin can dephosphorylate myopodin.

**Dephosphorylation of myopodin by calcineurin abrogates 14-3-3 binding.** To determine whether the dephosphorylation of myopodin by calcineurin abrogates the myopodin-14-3- $\beta$  interaction, 1  $\mu$ g of purified FLAG-myopodin was dephosphorylated with  $\lambda$ -PPase or CnA at 30°C for 30 min and incubated with immobilized GST-14-3- $\beta$ . Myopodin binding was then analyzed by immunoblotting using an anti-FLAG antibody. As previously described (11), the absence of phosphatase treatment resulted in a strong and specific binding of phosphorylated myopodin to GST-14-3- $\beta$ , whereas dephosphorylation by  $\lambda$ -PPase abrogated the myopodin-14-3-3 interaction (Fig. 4C). Similarly, the dephosphorylation of myopodin by CnA abrogated the 14-3- $\beta$  binding in a concentration-dependent fashion (Fig. 4C). One unit of CnA significantly reduced the myopodin-14-3- $\beta$  interaction, whereas dephosphorylation of myopodin with 2 units of CnA abrogated 14-3-3 binding (Fig. 4C). Together, myopodin is a novel direct substrate of calcineurin, and dephosphorylation of myopodin by calcineurin prevents the myopodin-14-3- $\beta$  interaction. To test whether both phospho-acceptor and 14-3-3-binding sites within myopodin serve as calcineurin substrates, we repeated the GST-binding assay using the FLAG-myopodin mutants S225D, T272E, and S225DT272E (Fig. 5). As shown before, calcineurin treatment of wild-type myopodin abrogated 14-3-3 binding, whereas the ability of the double mutant S225DT272E to bind 14-3-3 was not affected by calcineurin (Fig. 5, right panels). In contrast, when phosphorylation was only mimicked on either one of the two residues (S225D or T272E), weak 14-3-3 binding could be detected (Fig. 5). Altogether, these results show that S225 and T272 both serve as calcineurin substrates.

**PKA and CaMKII promote the nuclear import of myopodin in C2C12 myoblasts.** The nuclear import of myopodin requires the phosphorylation of S225 and T272 (11). Both residues can be phosphorylated by PKA and CaMKII (Fig. 2 and 3). This raises the intriguing possibility that the phosphorylation by PKA and CaMKII controls the nuclear import of myopodin.

To test this hypothesis, we analyzed the effect of specific PKA and CaMKII inhibitors on the subcellular localization of myopodin in C2C12 myoblasts by double-labeling deconvolution microscopy with 4',6'-diamidino-2-phenylindole (DAPI) (Fig. 6). As expected from previous studies (43), control cells displayed a virtually exclusive nuclear localization of myopodin. The inhibition of CaMKII by KN62 slightly reduced the nuclear import of myopodin (Fig. 6A). The inhibition of PKA by H89, KT5720, or Rp-cAMP significantly reduced the nuclear import of myopodin, and the combined application of H89 and KN62 completely suppressed the nuclear import of myopodin. In contrast, the inhibition of phosphatidylinositol-3-kinase (PI3K) by wortmannin or PKC $\alpha$  by Ro31-8220 did not interfere with the nuclear import of myopodin (Fig. 6A). The quantitative analysis (Fig. 6B) showed that in the control groups, 97.0  $\pm$  2.0% of counted cells displayed N>C myopodin, compared with 75.3  $\pm$  5.0% after KN62, 0  $\pm$  0.0% after H89, KN62 plus H89, KT5720, or Rp-cAMP treatment versus 95.0  $\pm$  2.6% after Ro31-8220 and 96.7  $\pm$  2.1% after wortmannin treatment ( $P$  < 0.0001, ANOVA). In concert, PKA and CaMKII activities are required for the efficient nuclear import of myopodin in C2C12 myoblasts, whereas other serine/threonine kinases, such as PI3K or PKC $\alpha$ , are not involved in the nuclear import of myopodin.

**Activation of PKA or inhibition of calcineurin induces the nuclear import of myopodin in adult cardiac myocytes.** In undifferentiated myoblasts, myopodin is localized in the nucleus (43), and the nuclear import of myopodin requires its phosphorylation by PKA (Fig. 6). In contrast, in differentiated myotubes, myopodin is found at the cytoplasmic Z-disc and only translocates into the nucleus during cellular stress (43). To test whether the nuclear import of myopodin in differentiated cardiac myocytes is also mediated by PKA signaling, we analyzed the localization of myopodin in isolated adult rat cardiac myocytes before and after activation of PKA. Under control conditions, we detected the colocalization of myopodin with  $\alpha$ -actinin at the Z-disc (Fig. 7A, upper panels). The combined application of IBMX and forskolin, which activates PKA by increasing cAMP levels, altered the subcellular localization of myopodin, and a partial reduction of myopodin at the Z-disc and a more diffuse localization around the Z-disc were detected by immunofluorescence microscopy. Most significantly, we also detected myopodin in the nucleus (Fig. 7A, middle panels). Similarly to myopodin, a fraction of 14-3- $\beta$  relocated to the nucleus after IBMX and forskolin treatment (Fig. 7B, middle panels), whereas mAKAP did not enter the nucleus (data not shown). Calcineurin dephosphorylates myopodin, thereby abrogating the myopodin-14-3- $\beta$  interaction (Fig. 4 and 5). Since the myopodin-14-3- $\beta$  interaction is required for importin  $\alpha$  binding and nuclear import (11), the inhibition of calcineurin by cyclosporine A (CsA) should induce the nuclear import of myopodin. Consistent with this hypothesis, we detected myopodin in the nucleus of cardiac myocytes after CsA treatment (Fig. 7A, lower panels). This effect was also seen for 14-3- $\beta$  (Fig. 7B, lower panels), but not for mAKAP (data not shown).

**Overexpression of  $\alpha$ -actinin prevents the nuclear import of myopodin.** In undifferentiated myoblasts that do not express  $\alpha$ -actinin (26), myopodin is found in the nucleus (43). In contrast, in differentiated myocytes myopodin colocalizes with

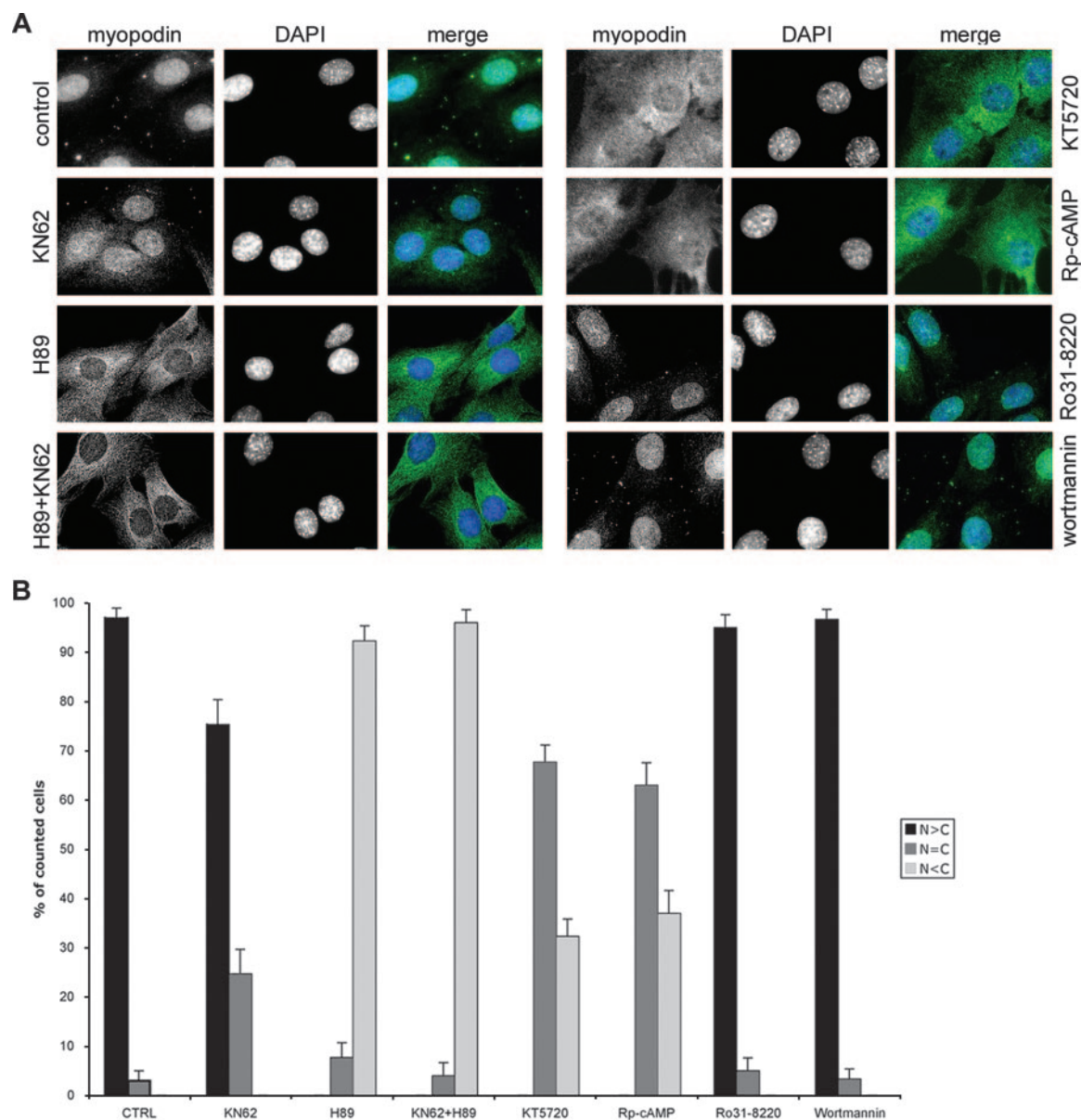


FIG. 6. PKA, CaMKII, and calcineurin regulate the nuclear import of myopodin. (A) In undifferentiated dimethyl sulfoxide (DMSO)-treated C2C12 myoblasts (control), myopodin is localized in the nucleus, as revealed by double-labeling deconvolution microscopy with DAPI. Pharmacological inhibition of CaMKII by KN62 partially reduces the nuclear import of myopodin, leading to the appearance of myopodin in the cytoplasm. The PKA inhibitors H89, KT5720, and Rp-cAMP significantly impair nuclear import of myopodin, whereas the combined inhibition of PKA and CaMKII abrogates the nuclear import of myopodin. In contrast, inhibition of PI3K by wortmannin or PKC $\alpha$  by Ro31-8220 does not interfere with the nuclear import of myopodin. (B) Quantitative analysis showing a significant reduction in the number of nuclear (N>C) myopodin-displaying cells and a concomitant increase in the number of cytoplasmic (N<C) myopodin-displaying cells after PKA inhibition (H89, KT5720, and Rp-cAMP) compared to DMSO-treated cells (CTRL). CaMKII inhibition (KN62) also significantly decreases the number of cells with mainly nuclear myopodin, but in contrast to PKA inhibition, KN62 significantly increased the number of cells displaying equally distributed (N=C) myopodin. Wortmannin and Ro31-8220 did not alter the nuclear localization of myopodin. Statistical significance was confirmed by analysis of variance between groups ( $P < 0.001$ ).

$\alpha$ -actinin at the Z-disc (43), and both proteins biochemically interact in the heart (Fig. 1). This prompted us to test whether the binding to  $\alpha$ -actinin anchors myopodin in the cytoplasm, thereby preventing its nuclear import. Consistent with this hypothesis, the transfection of undifferentiated myoblasts with FLAG- $\alpha$ -actinin-2 but not with FLAG-14-3-3 $\beta$ , serving as a control, caused the reduction of nuclear myopodin labeling

and its accumulation in the cytoplasm, where it colocalized with FLAG- $\alpha$ -actinin-2 (Fig. 8A). These findings suggest that in adult myocytes,  $\alpha$ -actinin anchors myopodin at the Z-disc. To test whether the phosphorylation-dependent binding of 14-3-3 to myopodin could override the  $\alpha$ -actinin-mediated cytoplasmic anchorage of myopodin, C2C12 myoblasts were cotransfected with GFP-myopodin and FLAG- $\alpha$ -actinin-2 (Fig.



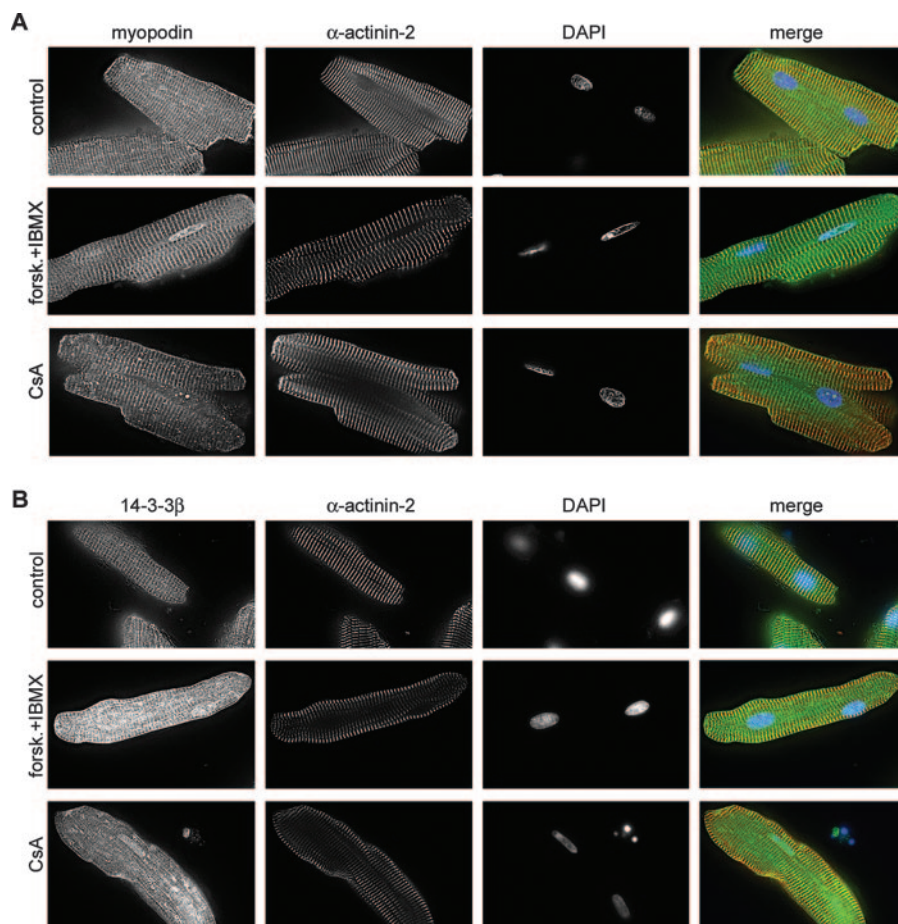


FIG. 7. The subcellular localization of myopodin in cardiac myocytes is regulated by cAMP and calcineurin activity. (A) In untreated isolated adult rat cardiac myocytes (control), myopodin colocalizes with  $\alpha$ -actinin at the Z-disc. Activation of PKA by forskolin (forsk.) and IBMX or inhibition of calcineurin by CsA causes the partial release of myopodin from the Z-disc and subsequent nuclear import. (B) 14-3-3 $\beta$  partially colocalizes with  $\alpha$ -actinin at the Z-disc of control cells. Similarly to myopodin, a fraction of 14-3-3 $\beta$  relocates into the nucleus after activation of PKA or inhibition of calcineurin.

8B). In the absence of  $\alpha$ -actinin, wild-type GFP-myopodin was mainly detected in the nucleus, whereas the coexpression of FLAG- $\alpha$ -actinin-2 caused its cytoplasmic redistribution, an effect similar to the one observed for endogenous myopodin (Fig. 8A). In contrast, when the myopodin mutant S225DT272E was used as the GFP-fusion protein, FLAG- $\alpha$ -actinin-2 coexpression did not result in the cytoplasmic localization of myopodin, and GFP-myopodin showed unaltered nuclear localization (Fig. 8B). Based on our previous findings that S225AT272E binds 14-3-3 constitutively (11), we conclude that the phosphorylation-dependent binding of 14-3-3 to myopodin can override the  $\alpha$ -actinin-mediated cytoplasmic anchorage of myopodin.

**14-3-3 $\beta$  and  $\alpha$ -actinin compete for myopodin binding.** Myopodin can bind to both 14-3-3 $\beta$  (11) and  $\alpha$ -actinin (Fig. 1), but only the interaction with 14-3-3 is regulated by the phosphorylation of myopodin. To test the hypothesis that 14-3-3 and  $\alpha$ -actinin compete for myopodin binding, we reconstituted a trimeric protein complex with purified proteins (Fig. 8C). When 1  $\mu$ g of FLAG-myopodin was incubated with 1  $\mu$ g of immobilized GST-14-3-3 $\beta$  (Fig. 8C, left panel), we detected the interaction between the two proteins as has been reported

elsewhere (11). However, when increasing amounts of purified FLAG- $\alpha$ -actinin-2 (0.1 to 1.0  $\mu$ g) were added to the assay mixture, the binding of 14-3-3 $\beta$  to myopodin decreased in a concentration-dependent fashion. No myopodin-14-3-3 $\beta$  interaction was detected with the presence of 1  $\mu$ g of  $\alpha$ -actinin-2 (Fig. 8C, left panel). Since  $\alpha$ -actinin-2 and 14-3-3 $\beta$  do not interact with each other, the loss of myopodin binding to 14-3-3 $\beta$  results from the increased binding of  $\alpha$ -actinin to myopodin. In a converse experiment, the addition of increasing amounts of FLAG-14-3-3 $\beta$  (0.1 to 1.0  $\mu$ g) gradually decreased the binding of FLAG-myopodin to GST- $\alpha$ -actinin-2 (Fig. 8C, middle panel). Again, we detected no binding of 14-3-3 to  $\alpha$ -actinin, thereby confirming that the observed loss of  $\alpha$ -actinin binding to myopodin is caused by the interaction of myopodin with 14-3-3 $\beta$ .

## DISCUSSION

The present study identifies the Z-disc protein myopodin as a novel direct target of PKA, CaMKII, and calcineurin signaling in the heart. These enzymes regulate the phosphorylation state of myopodin, thereby controlling the subcellular localiza-

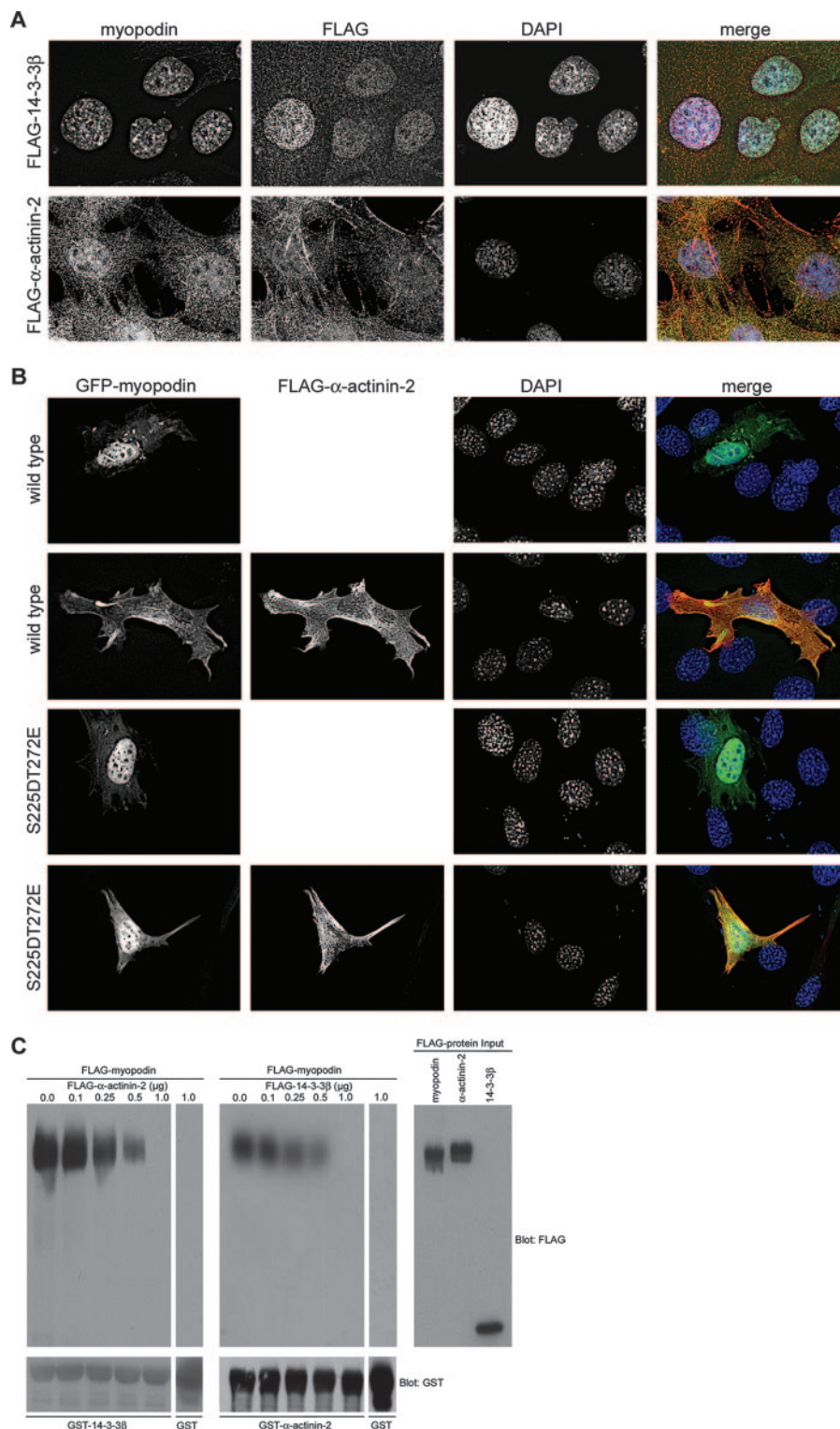


FIG. 8.  $\alpha$ -Actinin competes with 14-3-3 $\beta$  for myopodin binding and anchors myopodin in the cytoplasm. (A) Transfection of FLAG- $\alpha$ -actinin-2 but not FLAG-14-3-3 $\beta$  causes the cytoplasmic retention of endogenous myopodin in undifferentiated C2C12 myoblasts. (B) Coexpression of FLAG- $\alpha$ -actinin-2 with GFP-myopodin in C2C12 myoblasts causes the cytoplasmic localization of wild-type myopodin, but not of the S225DT272E mutant, which is still targeted to the nucleus. In the absence of FLAG- $\alpha$ -actinin-2, both GFP-myopodin forms are localized in the nucleus. (C) FLAG- $\alpha$ -actinin-2 induces the concentration-dependent loss of FLAG-myopodin binding to GST-14-3-3 $\beta$  (left panels). Conversely, FLAG-14-3-3 $\beta$  causes the concentration-dependent loss of FLAG-myopodin binding to GST- $\alpha$ -actinin-2 (right panels).

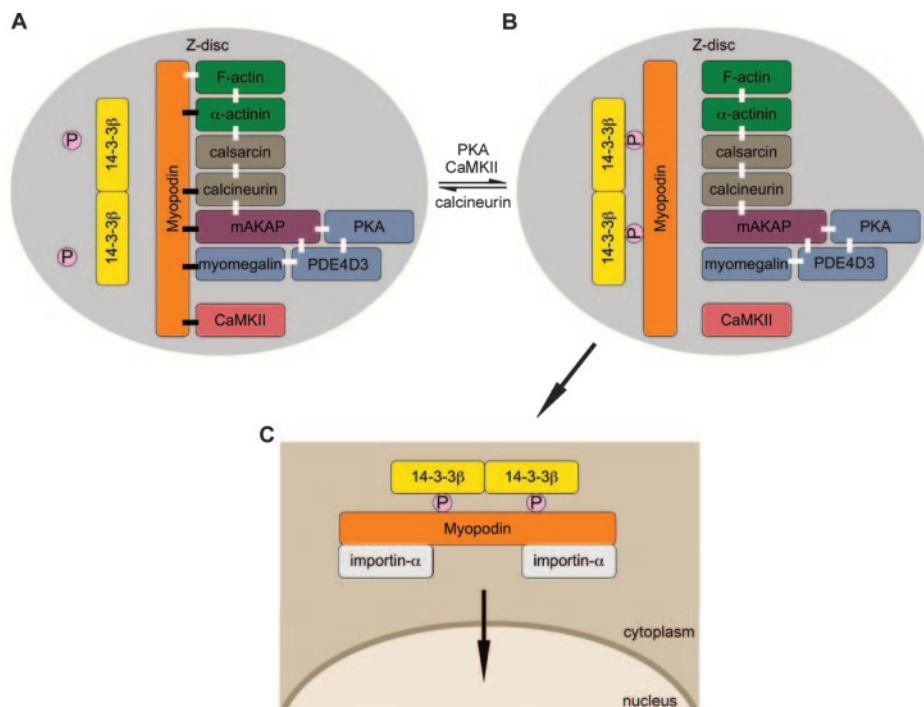


FIG. 9. Model for the regulation of myopodin's subcellular localization in cardiac myocytes. (A) Under normal conditions, myopodin is tethered to the Z-disc of differentiated cardiac myocytes, where it is part of a signal transduction unit. The complex contains structural (actin and  $\alpha$ -actinin), signaling (PKA, CaMKII, calcineurin, calsarcin, and PDE4D3), and scaffolding (mAKAP and myomegalin) proteins. White bars indicate previously published interactions, and black bars show interactions identified in this study. Calcineurin keeps myopodin dephosphorylated, and 14-3-3 cannot directly bind to myopodin. (B) Upon activation of PKA/CaMKII or inhibition of calcineurin, myopodin undergoes phosphorylation, thereby enabling its interaction with 14-3-3, which in turn causes the release of myopodin from Z-disc-anchoring proteins like  $\alpha$ -actinin. (C) After release from the Z-disc, 14-3-3-bound myopodin can interact with the cytoplasmic nuclear import receptor importin  $\alpha$  and enter the nucleus.

tion of myopodin in adult cardiac myocytes (Fig. 9). These results support the idea that myopodin serves as a messenger in a unique intracellular signaling pathway, whereby changes in Z-disc dynamics may translate into altered nuclear function during cardiac development and remodeling.

Recently, it has been suggested that Z-disc proteins, in addition to their structural function, participate in intracellular signaling pathways (13). Work from several groups provided evidence that the Z-disc of cardiac myocytes may serve as a mechanosensor during myocyte differentiation and cardiac remodeling (13). Specifically, it was proposed that the Z-disc is a signal transduction unit that communicates with the nucleus. In this scenario the Z-disc would sense an increase in the mechanical load of the heart and respond by sending a signal to the nucleus. This signal would in turn alter gene expression of muscle-specific proteins, leading to cardiac hypertrophy and remodeling (36). Clearly, such pathways would require messengers that can shuttle between the Z-disc and the nucleus. Several proteins meet these criteria and therefore could function as potential signal transducers between the two compartments. For example, LIM domain-containing proteins, like FHL2 and FHL3 (12, 31), zyxin (20), and the muscle LIM protein (MLP) (23), can shuttle between the cytosol and the nucleus of myocytes in a differentiation- and stress-dependent manner. MLP, also called CRP3 (cystein-rich protein), and other members of the CRP protein family (CRP1 and CRP2) have also been proposed to function as stress and damage

sensors at the actin cytoskeleton (18). Upon activation, CRPs translocate into the nucleus, where they can activate the expression of muscle-specific genes, resulting in muscle repair (18). However, the molecular mechanisms regulating the intracellular shuttling of LIM domain proteins have yet to be elucidated.

Myopodin does not contain a LIM domain, but it shares several key features with LIM proteins. Similar to LIM proteins, myopodin directly binds to  $\alpha$ -actinin, which anchors myopodin at the Z-disc. More importantly, myopodin also shuttles between the Z-disc and the nucleus in a differentiation- and stress-dependent fashion (43), thus making it a good candidate as a signaling intermediary between both compartments. We recently demonstrated that serine/threonine phosphorylation-dependent binding of myopodin to 14-3-3 is necessary and sufficient for the interaction between myopodin and importin  $\alpha$  (11), but the protein kinase(s) which phosphorylates myopodin remained unknown. The present study shows that myopodin is part of a multiprotein signal transduction unit that also includes PKA and CaMKII. Both kinases can phosphorylate the 14-3-3-binding motifs of myopodin, thereby enabling the binding of myopodin to 14-3-3. Similar to the biochemical inhibition of 14-3-3 binding (11), the pharmacological inhibition of PKA and CaMKII abrogates the nuclear import of myopodin in myoblasts. Moreover, in adult cardiac myocytes the activation of PKA induces the release of myopodin from the Z-disc and results in its nuclear import. It should be noted

that the differences between the *in vitro* and *in vivo* phosphorylation data imply that myopodin harbors additional PKA and CaMKII phosphorylation sites, which remain to be identified. These sites may also participate in the regulation of the nuclear import of myopodin. Such a function could explain the observed differential effects of PKA and CaMKII inhibition on the subcellular localization of myopodin. The observed discrepancy between the *in vitro* and *in vivo* phosphorylation experiments using PKA and CaMKII might be due to the fact that both kinases act cooperatively on the two 14-3-3-binding sites or in combination with other unidentified protein kinases. Clearly, future studies will be required to test this hypothesis.

This study also reveals that 14-3-3 proteins can modulate the binding of myopodin to its interacting proteins in several ways. 14-3-3 binding enables not only the interaction between myopodin and importin  $\alpha$  in a cooperative fashion (11) but also competitively abrogates the interaction between myopodin and  $\alpha$ -actinin. In undifferentiated myoblasts that do not express  $\alpha$ -actinin (26), myopodin is imported into the nucleus (43). In contrast, when  $\alpha$ -actinin is overexpressed in these cells, myopodin is sequestered in the cytoplasm, where it colocalizes with  $\alpha$ -actinin. However, this  $\alpha$ -actinin-mediated cytoplasmic anchorage of myopodin is overridden when myopodin is mutated, in that it can bind 14-3-3 constitutively. These results support the idea that  $\alpha$ -actinin serves as a cytoplasmic anchor of myopodin, which is antagonized by 14-3-3 binding, resulting in the nuclear import of myopodin. This idea is in keeping with the results of the binding assays showing that increasing amounts of 14-3-3 decrease the binding of  $\alpha$ -actinin to myopodin and vice versa, thereby explaining the negative effect of  $\alpha$ -actinin on the nuclear import of myopodin. Such an  $\alpha$ -actinin-mediated cytoplasmic anchoring mechanism in striated myocytes has been proposed before in that it regulates the subcellular localization of CRPs (3). Of note, the present study is the first to identify such a mechanism on a molecular level.

Several lines of evidence support the notion that signaling events leading to the development of cardiac hypertrophy can be modulated by mAKAP signaling units that contain PKA, the cAMP-responsive guanine nucleotide exchange factor EPAC, and phosphodiesterase 4 (PDE4) (29). In the current study we identified mAKAP (19) as another component of the myopodin signaling complex, thereby linking mAKAP signaling to the Z-disc. In addition to PKA, AKAPs can also bind to PDEs (29), enzymes that degrade cyclic nucleotides like cAMP. cAMP is synthesized by adenylate cyclases at the plasma membrane and diffuses into the cytosol to activate downstream effectors like PKA (29). By anchoring PDEs at specific sites, the cellular action of cAMP can be controlled spatially and temporally (17), and the coanchoring of PKA and PDEs enables a tight regulation of PKA signaling. The cAMP-specific PDE4 subfamily is highly expressed in the heart (30). PDE4 consists of about 16 distinct isoforms, and the mAKAP-anchored isoform is PDE4D3 (7). A previous yeast two-hybrid screen using PDE4D3 as bait identified a novel protein named myomegalin (42). We have now identified myomegalin as myopodin-interacting protein. Hence, myopodin can interact with two PDE4D3-anchoring proteins, mAKAP and myomegalin. Furthermore, myopodin exists in a complex with PKA via mAKAP and serves as a PKA substrate. Together these findings raise the intriguing possibility that in the heart, cAMP

signaling tightly regulates not only the phosphorylation of myopodin but also its subcellular localization. Consistently, the increase of cAMP levels in adult cardiac myocytes by simultaneous activation of adenylate cyclases and inhibition of PDEs lead to the nuclear import of myopodin and 14-3-3 $\beta$ .

The present study has also identified myopodin as a novel direct target of calcineurin. In adult cardiac myocytes, a fraction of the calcineurin pool is anchored at the Z-disc via interactions with calsarcins/ $\alpha$ -actinin (14) or MLP (16). Thus far, only a few substrates of calcineurin have been described, including the NFAT family of transcription factors (6, 28). Interestingly, NFATc is also localized at the Z-disc of resting myocytes. Upon electric stimulation it translocates into the nucleus, where it activates prohypertrophic gene programs (27). Of note, the nuclear translocation and full transcriptional activity of NFAT requires its dephosphorylation by calcineurin (6) as well as the activation of the mAKAP signaling complex (34) and the release of NFAT from 14-3-3 binding (4). The experiments described herein imply that myopodin not only directly interacts with calcineurin but also indirectly via the calcineurin-binding proteins mAKAP (34) and calsarcins/ $\alpha$ -actinin (14). Calcineurin dephosphorylates myopodin and thereby abrogates the myopodin–14-3-3 interaction. Conversely, the inhibition of calcineurin by CsA causes the release from the Z-disc and the nuclear import of myopodin. Hence, the dephosphorylation by calcineurin is required for the anchorage of myopodin at the Z-disc. In concert, these results suggest that calcineurin is a general regulator of signaling protein targeting. It will be interesting to see whether in addition to NFAT and myopodin the subcellular localization of other proteins in the heart or elsewhere is also controlled by calcineurin. Of note, similar to NFAT (15), myopodin only interacts with the activated form of CnA. However, in contrast to NFAT and most other known calcineurin target proteins, myopodin lacks a consensus (PxIxIT) calcineurin docking site (15). Clearly, future studies will be required to map the calcineurin-binding site(s) in myopodin.

Altogether, we identified a novel Z-disc signal transduction unit that communicates with the nucleus of cardiac myocytes by regulating the phosphorylation state of myopodin. Our results highlight how phosphorylation and dephosphorylation events can dynamically modulate the composition of large multiprotein signaling complexes (Fig. 9). Such complexes contain signaling and scaffolding proteins as well as mobile signal mediators like myopodin, whose access to or release from these complexes is tightly regulated by external or internal cues (35). The regulated presence or absence of a mediator can either alter the function of the complex or influence a target outside the complex. The identification of myopodin as a direct target of PKA, CaMKII, and calcineurin defines a novel intracellular signaling pathway, whereby changes in Z-disc dynamics may alter nuclear function during cardiac development and remodeling and may open new therapeutic modalities for the prevention or treatment of cardiac failure by the modulation of myopodin signaling.

#### ACKNOWLEDGMENTS

We thank Mary Donnelly, Celine Chiu, Eric Chan, Frank Graner, and Svetlana Ratner for excellent technical assistance, Hoon Young Choi for help with statistical analysis, and Stefan Hüttelmaier, Uni-

versity of Halle-Wittenberg, Halle, Germany, for advice on the phosphorylation assays. We also thank Norbert Frey, University of Heidelberg, Heidelberg, Germany, and Eric N. Olson, University of Texas, Southwestern Medical Center, Dallas, as well as Thomas R. Soderling and John D. Scott, The Vollum Institute, Oregon Health & Science University, Portland, for providing cDNA constructs.

This work was supported by National Institutes of Health grants DA18886, DK57683, and DK062472 to P.M. and HL73458 to A.D.S.

#### REFERENCES

- Asanuma, K., K. Kim, J. Oh, L. Giardino, S. Chabanis, C. Faul, J. Reiser, and P. Mundel. 2005. Synaptopodin regulates the actin-bundling activity of alpha-actinin in an isoform-specific manner. *J. Clin. Invest.* **115**:1188–1198.
- Asanuma, K., E. Yanagida-Asanuma, C. Faul, Y. Tomino, K. Kim, and P. Mundel. 2006. Synaptopodin orchestrates actin organization and cell motility via regulation of RhoA signalling. *Nat. Cell Biol.* **8**:485–491.
- Beckerle, M. C. 1997. Zyxin: zinc fingers at sites of cell adhesion. *Bioessays* **19**:949–957.
- Chow, C. W., and R. J. Davis. 2000. Integration of calcium and cyclic AMP signaling pathways by 14-3-3. *Mol. Cell Biol.* **20**:702–712.
- Clark, K. A., A. S. McElhinny, M. C. Beckerle, and C. C. Gregorio. 2002. Striated muscle cytoarchitecture: an intricate web of form and function. *Annu. Rev. Cell. Dev. Biol.* **18**:637–706.
- Crabtree, G. R., and E. N. Olson. 2002. NFAT signaling: choreographing the social lives of cells. *Cell* **109**(Suppl.):S67–S79.
- Dodge, K. L., S. Khouangathiene, M. S. Kafiloff, R. Mouton, E. V. Hill, M. D. Houslay, L. K. Langeberg, and J. D. Scott. 2001. mA KAP assembles a protein kinase A/PDE4 phosphodiesterase cAMP signaling module. *EMBO J.* **20**:1921–1930.
- Dougherty, M. K., and D. K. Morrison. 2004. Unlocking the code of 14-3-3. *J. Cell Sci.* **117**:1875–1884.
- Epstein, N. D., and J. S. Davis. 2003. Sensing stretch is fundamental. *Cell* **112**:147–150.
- Ervasti, J. M. 2003. Costameres: the Achilles' heel of Herculean muscle. *J. Biol. Chem.* **278**:13591–13594.
- Faul, C., S. Huttelmaier, J. Oh, V. Hachet, R. H. Singer, and P. Mundel. 2005. Promotion of importin  $\alpha$ -mediated nuclear import by the phosphorylation-dependent binding of cargo protein to 14-3-3. *J. Cell Biol.* **169**:415–424.
- Fimia, G. M., D. De Cesare, and P. Sassone-Corsi. 2000. A family of LIM-only transcriptional coactivators: tissue-specific expression and selective activation of CREB and CREM. *Mol. Cell Biol.* **20**:8613–8622.
- Frank, D., C. Kuhn, H. A. Katus, and N. Frey. 2006. The sarcomeric Z-disc: a nodal point in signalling and disease. *J. Mol. Med.* **84**:446–468.
- Frey, N., J. A. Richardson, and E. N. Olson. 2000. Calcineurins, a novel family of sarcomeric calcineurin-binding proteins. *Proc. Natl. Acad. Sci. USA* **97**:14632–14637.
- Garcia-Cozar, F. J., H. Okamura, J. F. Aramburu, K. T. Shaw, L. Pelletier, R. Showalter, E. Villafranca, and A. Rao. 1998. Two-site interaction of nuclear factor of activated T cells with activated calcineurin. *J. Biol. Chem.* **273**:23877–23883.
- Heineke, J., H. Ruetten, C. Willenbockel, S. C. Gross, M. Naguib, A. Schaefer, T. Kempf, D. Hilfiker-Kleiner, P. Caroni, T. Kraft, R. A. Kaiser, J. D. Molkentin, H. Drexler, and K. C. Wollert. 2005. Attenuation of cardiac remodeling after myocardial infarction by muscle LIM protein-calcineurin signaling at the sarcomeric Z-disc. *Proc. Natl. Acad. Sci. USA* **102**:1655–1660.
- Houslay, M. D., and D. R. Adams. 2003. PDE4 cAMP phosphodiesterases: modular enzymes that orchestrate signalling cross-talk, desensitization and compartmentalization. *Biochem. J.* **370**:1–18.
- Kadmas, J. L., and M. C. Beckerle. 2004. The LIM domain: from the cytoskeleton to the nucleus. *Nat. Rev. Mol. Cell Biol.* **5**:920–931.
- Kapiloff, M. S., R. V. Schillace, A. M. Westphal, and J. D. Scott. 1999. mA KAP: an A-kinase anchoring protein targeted to the nuclear membrane of differentiated myocytes. *J. Cell Sci.* **112**:2725–2736.
- Kato, T., J. Muraski, Y. Chen, Y. Tsujita, J. Wall, C. C. Glembotski, E. Schaefer, M. Beckerle, and M. A. Sussman. 2005. Atrial natriuretic peptide promotes cardiomyocyte survival by cGMP-dependent nuclear accumulation of zyxin and Akt. *J. Clin. Invest.* **115**:2716–2730.
- Klee, C. B., H. Ren, and X. Wang. 1998. Regulation of the calmodulin-stimulated protein phosphatase, calcineurin. *J. Biol. Chem.* **273**:13367–13370.
- Knoll, R., M. Hoshijima, H. M. Hoffman, V. Person, I. Lorenzen-Schmidt, M. L. Bang, T. Hayashi, N. Shiga, H. Yasukawa, W. Schaper, W. McKenna, M. Yokoyama, N. J. Schork, J. H. Omens, A. D. McCulloch, A. Kimura, C. C. Gregorio, W. Poller, J. Schaper, H. P. Schultheiss, and K. R. Chien. 2002. The cardiac mechanical stretch sensor machinery involves a Z disc complex that is defective in a subset of human dilated cardiomyopathy. *Cell* **111**:943–955.
- Kong, Y., M. J. Flick, A. J. Kudla, and S. F. Konieczny. 1997. Muscle LIM protein promotes myogenesis by enhancing the activity of MyoD. *Mol. Cell Biol.* **17**:4750–4760.
- Lafamme, M. A., and P. L. Becker. 1999. G(s) and adenylyl cyclase in transverse tubules of heart: implications for cAMP-dependent signaling. *Am. J. Physiol.* **277**:H1841–H1848.
- Lange, S., E. Ehler, and M. Gautel. 2006. From A to Z and back? Multi-compartment proteins in the sarcomere. *Trends Cell Biol.* **16**:11–18.
- Lin, Z., M. H. Lu, T. Schultheiss, J. Choi, S. Holtzer, C. DiLullo, D. A. Fischman, and H. Holtzer. 1994. Sequential appearance of muscle-specific proteins in myoblasts as a function of time after cell division: evidence for a conserved myoblast differentiation program in skeletal muscle. *Cell Motil. Cytoskel.* **29**:1–19.
- Liu, Y., Z. Csereny, W. R. Randall, and M. F. Schneider. 2001. Activity-dependent nuclear translocation and intranuclear distribution of NFATc in adult skeletal muscle fibers. *J. Cell Biol.* **155**:27–40.
- Macian, F. 2005. NFAT proteins: key regulators of T-cell development and function. *Nat. Rev. Immunol.* **5**:472–484.
- McConnachie, G., L. K. Langeberg, and J. D. Scott. 2006. AKAP signaling complexes: getting to the heart of the matter. *Trends Mol. Med.* **12**:317–323.
- Mongillo, M., T. McSorley, S. Evellin, A. Sood, V. Lissandron, A. Terrin, E. Huston, A. Hannawacker, M. J. Lohse, T. Pozzan, M. D. Houslay, and M. Zaccolo. 2004. Fluorescence resonance energy transfer-based analysis of cAMP dynamics in live neonatal rat cardiac myocytes reveals distinct functions of compartmentalized phosphodiesterases. *Circ. Res.* **95**:67–75.
- Morgan, M. J., and A. J. Madgwick. 1999. The LIM proteins FHL1 and FHL3 are expressed differently in skeletal muscle. *Biochem. Biophys. Res. Commun.* **255**:245–250.
- O'Keefe, S. J., J. Tamura, R. L. Kincaid, M. J. Tocci, and E. A. O'Neill. 1992. FK-506- and CsA-sensitive activation of the interleukin-2 promoter by calcineurin. *Nature* **357**:692–694.
- Orr, A. W., B. P. Helmke, B. R. Blackman, and M. A. Schwartz. 2006. Mechanisms of mechanotransduction. *Dev. Cell* **10**:11–20.
- Pare, G. C., A. L. Bauman, M. McHenry, J. J. Michel, K. L. Dodge-Kafka, and M. S. Kapiloff. 2005. The mA KAP complex participates in the induction of cardiac myocyte hypertrophy by adrenergic receptor signaling. *J. Cell Sci.* **118**:5637–5646.
- Pawson, T., and J. D. Scott. 2005. Protein phosphorylation in signaling—50 years and counting. *Trends Biochem. Sci.* **30**:286–290.
- Pyle, W. G., and R. J. Solaro. 2004. At the crossroads of myocardial signaling: the role of Z-discs in intracellular signaling and cardiac function. *Circ. Res.* **94**:296–305.
- Pyo, R. T., J. Sui, A. Dhume, J. Palomeque, B. C. Blaxall, G. Diaz, J. Tunstead, D. E. Logothetis, R. J. Hajjar, and A. D. Schecter. 2006. CXCR4 modulates contractility in adult cardiac myocytes. *J. Mol. Cell. Cardiol.* **41**:834–844.
- Robson, R. M., D. E. Goll, N. Arakawa, and M. H. Stromer. 1970. Purification and properties of alpha-actinin from rabbit skeletal muscle. *Biochim. Biophys. Acta* **200**:296–318.
- Scott, J. D. 2006. Compartmentalized cAMP signalling: a personal perspective. *Biochem. Soc. Trans.* **34**:465–467.
- Sheng, T., S. Chi, X. Zhang, and J. Xie. 2006. Regulation of Gli1 localization by the cAMP/protein kinase A signaling axis through a site near the nuclear localization signal. *J. Biol. Chem.* **281**:9–12.
- Smith, F. D., and J. D. Scott. 2002. Signaling complexes: junctions on the intracellular information super highway. *Curr. Biol.* **12**:R32–R40.
- Verde, I., G. Pahlke, M. Salanova, G. Zhang, S. Wang, D. Coletti, J. Onuffer, S. L. Jin, and M. Conti. 2001. Myomegalin is a novel protein of the Golgi/centrosome that interacts with a cyclic nucleotide phosphodiesterase. *J. Biol. Chem.* **276**:11189–11198.
- Weins, A., K. Schwarz, C. Faul, L. Barisoni, W. A. Linke, and P. Mundel. 2001. Differentiation- and stress-dependent nuclear cytoplasmic redistribution of myopodin, a novel actin-bundling protein. *J. Cell Biol.* **155**:393–404.
- Zaccolo, M., T. Cesetti, G. Di Benedetto, M. Mongillo, V. Lissandron, A. Terrin, and I. Zamparo. 2005. Imaging the cAMP-dependent signal transduction pathway. *Biochem. Soc. Trans.* **33**:1323–1326.